energies

MDPI

Article

Permeabilities of Water–Oil Two-Phase Flow in Capillary Fractures with Different Wettabilities

Na Huang, Lei Liu *, Heng Chen and Yanyan Huang

State Key Laboratory of Multiphase Flow in Power Engineering, Xi'an Jiaotong University, Xi'an 710049, China; huangna1120@stu.xjtu.edu.cn (N.H.); 3122103095@stu.xjtu.edu.cn (H.C.); hyy3122303101@stu.xjtu.edu.cn (Y.H.)
* Correspondence: rliu@mail.xjtu.edu.cn

Abstract: The influence of wettability on the permeability performance of water–oil two-phase flow has attracted increasing attention. Dispersed flow and stratified flow are two flow regimes for water–oil two-phase flow in capillary fractures. The theoretical models of relative permeability considering wettability were developed for these two water–oil flow regimes from the momentum equations of the two-fluid model. Wettability coefficients were proposed to study the impact of wettability on relative permeabilities. Experiments were conducted to study the relative permeabilities of laminar water–oil two-phase flow in water-saturated and oil-saturated horizontal capillary fractures with different hydraulic diameters. These fractures were made of polymethylmethacrylate (PMMA) and polytetrafluoroethylene (PTFE), which had different surface wettabilities. In this experiment, the regimes are dispersed flow and stratified flow. The results show that the effect of wettability on the relative permeabilities increases as the hydraulic diameters of capillary fractures decrease for water–oil two-phase flow. The relative permeabilities in a water-saturated capillary fracture are higher than those in an oil-saturated capillary fracture of the same material. The relative permeabilities in a PTFE capillary fracture are larger than those in a PMMA capillary fracture under the same saturated condition. Wettability has little effect on the permeability performances of water–oil two-phase flow in water-saturated capillary fractures, but is significant for those in oil-saturated capillary fractures.

Keywords: relative permeability; wettability; water–oil flow; two-phase flow; capillary fracture; stratified flow; dispersed flow

check for updates

Citation: Huang, N.; Liu, L.; Chen, H.; Huang, Y. Permeabilities of Water–Oil Two-Phase Flow in Capillary Fractures with Different Wettabilities. *Energies* **2024**, *17*, 2353. https://doi.org/10.3390/en17102353

Academic Editor: Hossein Hamidi

Received: 2 April 2024
Revised: 5 May 2024
Accepted: 10 May 2024
Published: 13 May 2024

Copyright: © 2024 by the authors. Licensee MDPI, Basel, Switzerland. This article is an open access article distributed under the terms and conditions of the Creative Commons Attribution (CC BY) license (https://creativecommons.org/licenses/by/4.0/).

1. Introduction

Two-phase flow in capillary fractures has been received much attention in a lot of engineering fields such as ground water recharge, enhanced oil recovery, carbon dioxide sequestration, groundwater contamination and geothermal energy production [1]. Relative permeabilities are useful quantities to describe two-phase flow behaviors in capillary fractures and porous media [2]. The determination of relative permeabilities is of great significance for parameter calculation, dynamic analysis and reservoir numerical simulation [2,3]. Previous studies indicate that the relative permeabilities in capillary fractures are dependent on many factors such as fluid pressure, fracture geometry, flow regime, surface roughness, interfacial tension, and wettability [4–6]. Among these factors, wettability has attracted increasing attention.

Wettability is the ability of a liquid wetting on a solid surface. This parameter plays important roles in controlling fluid, solute, heat, and current flow in fractures and porous media [7]. For water–oil two-phase flow in capillary tubes, wettability influences the displacement efficiency and fluids' saturations by affecting relative permeabilities, since it is a significant factor in controlling multiphase flow [8]. Some researchers point out that wettability is related to the capillary effect, which not only affects gas–liquid two-phase flow [9,10], but also has an undeniable impact on liquid–liquid two-phase flow [5]. Therefore, the understanding of the wettability effect on water–oil two-phase flow in

capillary fractures has significance for fractured reservoirs. Generally, reservoirs have the following states of wettability, such as water saturated and oil saturated [11]. To date, few studies have been performed for the wettability effect on relative permeabilities in capillary fractures.

Some researchers have drawn the following conclusions through experiments. Zhao et al. [12] changed the wettability of a microfluidic porous medium and emphasized the significant effect of saturated condition on displacement efficiency via fluid-fluid displacement experiments. Paolinelli et al. [13] performed experiments of water–oil two-phase flow in carbon steel and PVC pipes of similar internal diameter 0.1 m. They demonstrated that poor surface wettability hindered droplet sticking and spreading in a hydrophobic pipe. Riley et al. [14] investigated water–oil flows in hydrophilic and hydrophobic channels. They found that the pressure drop of water–oil two-phase flow increased when oil completely or partially saturated the wall. Prakash et al. [15] examined the effect of capillary wall wettability on the liquid–liquid two-phase flow in a capillary tube with an inner diameter of 2.4 mm. They pointed out that the presence of a wetting layer or a thicker wetting film on a tube would affect the wettability of channel and the distribution of water–oil two-phase flow. Oyenowo et al. [16] experimentally studied the effect of aqueous formate solution on the core-scale wettability alteration of carbonate porous media and found that the fluid flowing in the porous media had an impact on the wettability of the cores. The initial oil-saturated core could reach a more water-saturated state by increasing the concentration of injected aqueous formate solution. These above experimental studies indicate that wettability situation has an important influence on water–oil two-phase flow.

Single and multiphase flow in fractures and porous media are commonly simulated by the pore-scale method. This method was also used to study the wettability effect on water–oil two-phase flow. Al-Futaisi et al. [17] used a two-phase pore network extracted from a sample of Bentheimer sandstone to investigate the influence of wettability alteration on two-phase flow. As the system became less water saturated, the residual oil saturation initially decreased but increased dramatically at the transition from water-saturated to oil-saturated condition and then decreased to a minimum in oil-saturated systems. Zhao et al. [18] studied the wettability effect on waterflood oil recovery based on a capillary-controlled pore-scale network model. Recovery increased as the system becomes less water saturated, whereas it initially increased and then decreased in oil-saturated systems. Ryazanov et al. [19] applied the pore-scale network model to make some quantitative predictions of residual oil in pore systems of mixed wettability. Residual oil was different when the system changed from moderately oil saturated to moderately water saturated. Zhao et al. [20] simulated water–oil two-phase flow in porous media with different oil-saturated solid fractions based on lattice Boltzmann model. At a constant water saturation, the relative permeability of water increased with the increase in the oil-saturated solid fraction. Cheng et al. [21] used a multi-relaxation time multi-component lattice Boltzmann method to investigate the wettability effect on the development of fingering flow in flat parallel plates. As saturated condition increased, finger flow increased and finger width decreased. Yi et al. [5] studied the two-phase flow in rough-walled fractures with different wettabilities based on the free energy multiphase lattice Boltzmann model. The wettability effect on fluid flow increased as the fracture width decreased. These above studies adopt numerical simulation and obtain conclusions similar to those of experimental studies on wettability.

As introduced above, the effects of wettability on water–oil two-phase flow have been extensively studied. These studies are either experimental or numerical simulation studies. There are few studies for different wettability situations such as water-saturated fractures and oil-saturated fractures, which are based on the combination of experiment and theory. In this work, the theoretical models of relative permeability considering wettability will be developed for water–oil flow from the momentum equations of the two-fluid model. Experiments were performed to verify the theoretical models developed.

2. Permeability Performance of Water–Oil Flow

The details of flow regimes are associated with wettability [13,22,23]. The water–oil flow regimes in channels of different hydraulic diameters were investigated by many researchers [24–28]. Core annular flow, dispersed flow, slug flow and stratified flow are four main flow regimes for water–oil two-phase flow in tubes and capillary fractures [28]. Dispersed flow and stratified flow are two common flow regimes occurring in capillary fractures [29]. The theoretical models of relative permeability considering wettability are developed for these two water–oil flow regimes from the momentum equations of the two-fluid model.

2.1. Absolute Permeability

The absolute permeability of laminar flow in capillary channels is shown as the followings [30]

$$k = \frac{2d_{\mathrm{h}}^2}{Po} \tag{1}$$

where k is absolute permeability, m^2; d_{h} is the hydraulic diameter of a fracture, m; Po is the Poiseuille number.

In Equation (1), the Poiseuille number for rectangular fractures is often predicted as below [31]

$$Po = 96\left(1 - 1.3553\alpha + 1.9467\alpha^2 - 1.7013\alpha^3 + 0.9564\alpha^4 - 0.2537\alpha^5\right) \tag{2}$$

where α is the aspect ratio of the shorter side and the longer side for a rectangular channel ($0 < \alpha \leq 1$).

In Equation (1), d_{h} is calculated as below

$$d_{\mathrm{h}} = \frac{4A}{B} \tag{3}$$

where A is the cross-sectional area, m^2; B is the wetted perimeter, m.

2.2. Relative Permeability

The relative permeabilities of water–oil two-phase flow in horizontal capillary channels are expressed as Equations (4) and (5) [32], which are

$$J_w = \frac{k_{rw}k}{\mu_w} \cdot \frac{\Delta p}{L} \tag{4}$$

$$J_{\mathrm{o}} = \frac{k_{\mathrm{ro}}k}{\mu_{\mathrm{o}}} \cdot \frac{\Delta p}{L} \tag{5}$$

where J_{w} and J_{o} are the seepage velocities for water and oil, respectively, m/s; k_{rw} is the relative permeability of water phase; k_{ro} is the relative permeability of the oil phase; μ_{w} is the dynamic viscosity of water phase, Pa·s; μ_{o} is the dynamic viscosity of the oil phase, Pa·s; L is the length of the capillary fracture, m. Δp is the pressure drop of water–oil flow, Pa.

From Equations (4) and (5), if the properties of fluids and a fracture are fixed, the relative permeabilities can be obtained for water–oil flow as long as the pressure drop is known at a certain flow rate. The pressure drop of water–oil flow in a capillary fracture is the key to study the seepage law of water–oil flow. When water and oil pass together in a capillary fracture, capillary force exists and is related to wettability [33]. The influence of wettability on the relative permeabilities of stratified and dispersed water–oil flow regimes in capillary fractures is analyzed in detail below.

For oil–water two-phase flow in capillary fractures, it can be assumed as one-dimensional steady flow. Assuming the phase 1 is a wetting fluid and the phase 2 is a non-wetting fluid, considering wall shear stresses, interfacial shear stress and capillary force, the momentum

equations can be obtained for laminar two-phase flow in a horizontal fracture according to the two-fluid model developed by Lahey [34]. The results are shown by the following Equations (6) and (7). The term $F_{\sigma 2}$ in Equation (7), which is related to capillary force, can be expressed by Equation (8) following the approach proposed for dispersed bubbles [34]. The sum of those terms associated with capillary force is zero by adding Equation (6) to Equation (7), which is expressed by Equation (9). Accordingly, the term $F_{\sigma 1}$ is obtained to be Equation (10). The main radius of curved surface for fluid 1 and 2 are denoted by r_1 and r_2. The interfacial tension between fluid 1 and 2 is denoted by σ. The term p_c in Equations (8) to (10) can be expressed by Equation (11).

$$-S_1 \frac{dp}{dx} = \frac{\tau_1 B_1}{A} - \frac{\tau_i B_i}{A} - F_{\sigma 1} \tag{6}$$

$$-S_2 \frac{d(p + p_c)}{dx} = \frac{\tau_2 B_2}{A} + \frac{\tau_i B_i}{A} + F_{\sigma 2} \tag{7}$$

$$F_{\sigma 2} = p_c \frac{dS_2}{dx} \tag{8}$$

$$F_{\sigma 2} + S_2 \frac{dp_c}{dx} - F_{\sigma 1} = 0 \tag{9}$$

$$F_{\sigma 1} = S_2 \frac{dp_c}{dx} + p_c \frac{dS_2}{dx} = \frac{d(S_2 p_c)}{dx} \tag{10}$$

$$p_c = \sigma \left(\frac{1}{r_1} + \frac{1}{r_2} \right) \tag{11}$$

The expressions of the variables in Equations (6) and (7) are relevant to flow regime. For stratified flow, Table 1 shows the basic relations for the calculations of those variables in Equations (6) and (7) [35].

Table 1. Basic relations for stratified flow.

Physical Quantity	Equation
Seepage velocity for fluid 1	$J_1 = S_1 u_1 = \frac{Q_1}{A} = \frac{\phi_1 Q}{A}$
Seepage velocity for fluid 2	$J_2 = S_2 u_2 = \frac{Q_2}{A} = \frac{\phi_2 Q}{A}$
Wall shear stress for fluid 1	$\tau_1 = \frac{1}{8} \lambda_1 \rho_1 u_1^2$
Wall shear stress for fluid 2	$\tau_2 = \frac{1}{8} \lambda_2 \rho_2 u_2^2$
Interfacial shear stress between fluids 1 and 2	$\tau_i = \frac{1}{8} \lambda_i \rho_i (u_2 - u_1) \lvert u_2 - u_1 \rvert$
Darcy friction coefficient for fluid 1	$\lambda_1 = \frac{Po}{Re_1}$
Darcy friction coefficient for fluid 2	$\lambda_2 = \frac{Po}{Re_2}$
Reynolds number for fluid 1	$Re_1 = \frac{u_1 \rho_1 d_1}{\mu_1}$
Reynolds number for fluid 2	$Re_2 = \frac{u_2 \rho_2 d_2}{\mu_2}$
Hydraulic diameters of fluids 1 and 2	$u_1 > u_2$, $d_1 = \frac{4A_1}{B_1 + B_i}$ $d_2 = \frac{4A_2}{B_2}$ $u_1 = u_2$, $d_1 = \frac{4A_1}{B_1}$ $d_2 = \frac{4A_2}{B_2}$ $u_1 < u_2$, $d_1 = \frac{4A_1}{B_1}$ $d_2 = \frac{4A_2}{B_2 + B_i}$

In Table 1, J_1 and J_2 are the seepage velocities for fluids 1 and 2, respectively, m/s; u_1 and u_2 are the average velocities for fluids 1 and 2, respectively, m/s; Q_1 is the volumetric flow rate of fluid 1, m^3/s; Q_2 is the volumetric flow rate of fluid 2, m^3/s; Q is the total volumetric flow rate of fluid 1 and fluid 2, m^3/s; ϕ_1 and ϕ_2 are the volumetric contents for fluid 1 and fluid 2, respectively. S_1 and S_2 are the saturations for fluid 1 and fluid 2, respectively. ρ_1 and ρ_2 are the densities for fluid 1 and fluid 2, respectively, kg/m^3; τ_1 and τ_2 are the wall shear stresses for fluid 1 and fluid 2, respectively, Pa; τ_i is the shear stress of two-phase interface, Pa; λ_1 and λ_2 are the Darcy friction factors for fluid 1 and fluid 2 in laminar case, respectively; λ_i and ρ_i are the friction factor and the density of faster phase, respectively; Re_1 and Re_2 are the Reynolds numbers of fluid 1 and fluid 2, respectively. A_1

and A_2 are the cross-sectional areas for fluid 1 and fluid 2, respectively, m^2; B_1 and B_2 are the wetted perimeters for fluid 1 and fluid 2, respectively, m; B_i is the wetted perimeter of two-phase interface, m; d_1 and d_2 are the hydraulic diameters of fluid 1 and fluid 2, respectively, m; μ_1 and μ_2 are the dynamic viscosities for fluid 1 and fluid 2, respectively, Pa·s; p_c is capillary pressure, Pa; $F_{\sigma 1}$ and $F_{\sigma 2}$ are the capillary forces for fluid 1 and fluid 2, respectively, Pa/m.

For stratified two-phase flow, the basic relations in Equations (6) and (7) are shown in Table 1. Equation (8), Equation (10) and the physical quantities in Table 1 are taken into Equations (6) and (7), Equations (12) and (13) are obtained as below

$$J_1 = S_1^3 \left(\frac{B}{B_1}\right)^2 a \left(1 + \frac{\frac{d(S_2 p_c)}{S_1 dx}}{\frac{\Delta p}{L}}\right) \frac{k}{\mu_1} \cdot \frac{\Delta p}{L} \tag{12}$$

$$J_2 = S_2^3 \left(\frac{B}{B_2}\right)^2 b \left(1 + \frac{-\frac{dp_c}{dx} - \frac{p_c}{S_2} \cdot \frac{dS_2}{dx}}{\frac{\Delta p}{L}}\right) \frac{k}{\mu_2} \cdot \frac{\Delta p}{L} \tag{13}$$

where a and b are interfacial slip coefficients of relative permeabilities for stratified flow, as shown in Table 2. These two interfacial slip coefficients were proposed to effectively reflect the influence of two-phase interfacial slip on the relative permeabilities of stratified flow in previous study [30].

Table 2. Interfacial slip coefficients.

	$u_1 = u_2$	$u_1 > u_2$	$u_1 < u_2$
a	1	$\frac{1}{\frac{(B_1+B_i)}{B_1}\left[1+\frac{B_i}{B_1}\left(1-\frac{\phi_2}{\phi_1}\cdot\frac{S_1}{S_2}\right)^2\right]}$	$\frac{1}{1-\frac{(B_2+B_i)B_i}{{B_1}^2}\cdot\frac{\mu_2}{\mu_1}\cdot\frac{\phi_2}{\phi_1}\cdot\left(\frac{S_1}{S_2}-\frac{\phi_1}{\phi_2}\right)^2}$
b	1	$\frac{1}{1-\frac{B_i(B_1+B_i)}{{B_2}^2}\cdot\frac{\mu_1}{\mu_2}\cdot\frac{\phi_1}{\phi_2}\cdot\left(\frac{S_2}{S_1}-\frac{\phi_2}{\phi_1}\right)^2}$	$\frac{1}{\frac{(B_2+B_i)}{B_2}\left[1+\frac{B_i}{B_2}\left(1-\frac{\phi_1}{\phi_2}\cdot\frac{S_2}{S_1}\right)^2\right]}$

From comparing Equations (4) and (5) with Equations (12) and (13), the relative permeabilities for stratified flow with the effect of wettability are obtained as follows

$$k_{r,1} = S_1^3 \left(\frac{B}{B_1}\right)^2 a \left(1 + \frac{\frac{d(S_2 p_c)}{S_1 dx}}{\frac{\Delta p}{L}}\right) = S_1^3 \left(\frac{B}{B_1}\right)^2 a(1 + c_1) \tag{14}$$

$$k_{r,2} = S_2^3 \left(\frac{B}{B_2}\right)^2 b \left(1 + \frac{-\frac{dp_c}{dx} - \frac{p_c}{S_2} \cdot \frac{dS_2}{dx}}{\frac{\Delta p}{L}}\right) = S_2^3 \left(\frac{B}{B_2}\right)^2 b(1 + c_2) \tag{15}$$

where $k_{r,1}$ is the relative permeability of wetting fluid 1, $k_{r,2}$ is the relative permeability of non-wetting fluid 2. c_1 is the wettability coefficient of the relative permeability of fluid 1. c_2 is the wettability coefficient of the relative permeability of fluid 2. These two proposed wettability coefficients are used to study the effect of wettability on the relative permeabilities.

From Equations (14) and (15), the relative permeabilities of stratified water–oil flow are relevant to wetted perimeter, saturation, interfacial slip coefficient and wettability coefficient. The relative permeabilities of stratified water–oil flow in a capillary fracture with the effect of wettability are shown in following Equations (16)–(19) in terms of the wettability coefficients. If oil is the wetting fluid and the water is non-wetting fluid, the expressions for stratified flow are the followings, which are

$$k_{r,1,o} = S_o^3 \left(\frac{B}{B_o}\right)^2 a(1 + c_{1,o}) \tag{16}$$

$$k_{r,2,w} = S_w^3 \left(\frac{B}{B_w} \right)^2 b(1 + c_{2,w}) \tag{17}$$

where $k_{r,1,o}$ is the relative permeability of oil in the case that oil is the wetting fluid, $c_{1,o}$ is the wettability coefficient of the relative permeability of oil in the case that oil is the wetting fluid, $k_{r,2,w}$ is the relative permeability of water in the case that water is the non-wetting fluid, $c_{2,w}$ is the wettability coefficient of the relative permeability of water in the case that water is the non-wetting fluid.

However, if water is the wetting fluid and oil is the non-wetting fluid, the equations are expressed for stratified flow as below

$$k_{r,2,o} = S_o^3 \left(\frac{B}{B_o} \right)^2 b(1 + c_{2,o}) \tag{18}$$

$$k_{r,1,w} = S_w^3 \left(\frac{B}{B_w} \right)^2 a(1 + c_{1,w}) \tag{19}$$

where $k_{r,2,o}$ is the relative permeability of oil in the case that oil is the non-wetting fluid, $c_{2,o}$ is the wettability coefficient of the relative permeability of oil in the case that oil is the non-wetting fluid, $k_{r,1,w}$ is the relative permeability of water in the case that water is the wetting fluid, $c_{1,w}$ is the wettability coefficient of the relative permeability of water in the case that water is the wetting fluid.

If wettability is not considered, Equations (20) and (21) are obtained. In this instance, the relative permeabilities of stratified water–oil flow are relevant to wetted perimeter, saturation and interfacial slip coefficient.

$$k_{ro} = S_o^3 \left(\frac{B}{B_o} \right)^2 a \tag{20}$$

$$k_{rw} = S_w^3 \left(\frac{B}{B_w} \right)^2 b \tag{21}$$

For dispersed flow, wall shear stress of non-wetting fluid 2 is zero, the wall shear stress of wetting fluid 1 is equal to the wall shear stress of dispersed flow, and the wetted perimeter for wetting fluid 1 is the total wetted perimeter. Equation (22) can be obtained from Equations (6) and (7) without considering wettability. The basic relations for dispersed flow are shown in Table 3 as below [36].

$$-S_2 \frac{dp}{dx} = \frac{\tau_i B_i}{A} = \frac{S_2 \tau_m B}{A} \tag{22}$$

Table 3. Basic relations for dispersed flow.

Physical Quantity	Equation
Wall shear stress for dispersed flow	$\tau_m = \frac{1}{8} \lambda_m \rho_m u_m^2$
Darcy friction coefficient for dispersed flow	$\lambda_m = \frac{p_o}{Re_m}$
Reynolds number for dispersed flow	$Re_m = \frac{u_m \rho_m d_h}{\mu_m}$
Density for two-phase flow	$\rho_m = \phi_1 \rho_1 + \phi_2 \rho_2 = S_1 \rho_1 + S_2 \rho_2$

In Table 3, τ_m is the wall shear stress for dispersed flow, Pa; λ_m is the Darcy friction factor for dispersed flow in laminar flow case; ρ_m is the density for dispersed flow, kg/m^3; Re_m is the Reynolds number of dispersed flow; μ_m is the dynamic viscosity for dispersed flow, Pa·s; u_m is the average velocity of dispersed flow, m/s.

Equation (22) and the physical quantities in Table 3 are taken into Equations (4) and (5), the relative permeabilities of dispersed water–oil flow in horizontal capillary fractures are

obtained, as shown in the following Equations (23) and (24). It can be seen that the relative permeabilities of dispersed water–oil flow are relevant to saturation and viscosity.

$$k_{\mathrm{ro}} = S_{\mathrm{o}} \frac{\mu_{\mathrm{o}}}{\mu_{\mathrm{m}}} \tag{23}$$

$$k_{\mathrm{rw}} = S_{\mathrm{w}} \frac{\mu_{\mathrm{w}}}{\mu_{\mathrm{m}}} \tag{24}$$

If wettability is considered, Equation (25) is obtained from Equations (6), (7) and (22). Equation (25) and the physical quantities in Table 3 are taken into Equations (4) and (5), the relative permeabilities of dispersed liquid–liquid flow in a capillary fracture with the effect of wettability are obtained as follows.

$$-\frac{dp}{dx} = \frac{\tau_{\mathrm{m}} B}{A}\left(1 - \frac{AF_{\sigma 1}}{S_1 \tau_{\mathrm{m}} B}\right) \tag{25}$$

$$k_{\mathrm{r1}} = S_1 \frac{\mu_1}{\mu_{\mathrm{m}}}\left(1 + \frac{\frac{d(S_2 p_{\mathrm{c}})}{dx}}{\frac{u_m \mu_{\mathrm{m}}}{k} - \frac{d(S_2 p_{\mathrm{c}})}{S_1 dx}}\right) = S_1 \frac{\mu_1}{\mu_{\mathrm{m}}}(1 + c_1) \tag{26}$$

$$k_{\mathrm{r2}} = S_2 \frac{\mu_2}{\mu_{\mathrm{m}}}\left(1 + \frac{\frac{d(S_2 p_{\mathrm{c}})}{dx}}{\frac{u_m \mu_{\mathrm{m}}}{k} - \frac{d(S_2 p_{\mathrm{c}})}{S_1 dx}}\right) = S_2 \frac{\mu_2}{\mu_{\mathrm{m}}}(1 + c_2) \tag{27}$$

From Equations (26) and (27), the relative permeability model for dispersed water–oil flow is related to saturation, viscosity and wettability coefficient. Similarly, the relative permeabilities of dispersed water–oil flow in a capillary fracture with the effect of wettability are shown in following Equations (28)–(31) in terms of the wettability coefficients. If oil is the wetting fluid and the water is non-wetting fluid, the expressions for dispersed water–oil flow are the followings.

$$k_{\mathrm{r,1,o}} = S_{\mathrm{o}} \frac{\mu_{\mathrm{o}}}{\mu_{\mathrm{m}}}(1 + c_{1,\mathrm{o}}) \tag{28}$$

$$k_{\mathrm{r,2,w}} = S_{\mathrm{w}} \frac{\mu_{\mathrm{w}}}{\mu_{\mathrm{m}}}(1 + c_{2,\mathrm{w}}) \tag{29}$$

However, if water is the wetting fluid and oil is the non-wetting fluid, the equations are expressed for dispersed water–oil flow as below.

$$k_{\mathrm{r,2,o}} = S_{\mathrm{o}} \frac{\mu_{\mathrm{o}}}{\mu_{\mathrm{m}}}(1 + c_{2,\mathrm{o}}) \tag{30}$$

$$k_{\mathrm{r,1,w}} = S_{\mathrm{w}} \frac{\mu_{\mathrm{w}}}{\mu_{\mathrm{m}}}(1 + c_{1,\mathrm{w}}) \tag{31}$$

3. Experimental Method and Setup

Considering that the laminar pore-scale flow satisfies Darcy's law, the relative permeabilities of laminar dispersed flow and stratified flow are investigated in this study for different wettability situations such as water-saturated capillary fractures and oil-saturated capillary fractures made of different materials.

3.1. Wettability of Fracture Materials

Solids with different wettabilities exhibit different surface properties, which lead to inconsistent liquid–liquid flow structures in channels [5]. It is generally believed that polymethylmethacrylate (PMMA) and polytetrafluoroethylene (PTFE) have different wettabilities. PMMA is hydrophilic and PTFE is hydrophobic. Solid wettability is often quantified by the contact angle. If one fluid contact angle is less than 90°, the solid is wetted by this fluid. The contact angle θ is the expression of thermodynamic equilibrium between

the liquid phase, the solid phase, and the gas phase, where the gas phase can be replaced by another immiscible liquid phase. It is shown as below [37]

$$\theta = \frac{\gamma_{sg} - \gamma_{sl}}{\gamma_{lg}} \tag{32}$$

where γ_{sg} is solid–gas surface tension, N/m; γ_{sl} is solid–liquid surface tension, N/m; γ_{lg} is liquid–gas surface tension, N/m.

A schematic of the contact angle of a liquid drop is shown in Figure 1. Water-saturated capillary fractures and oil-saturated capillary fractures have different wettability properties. In order to better comprehend the water–oil flow in a saturated capillary fracture, a liquid–liquid–solid contact angle is designed, as illustrated in Figure 2. The liquid–liquid–solid contact angle is measured in a transparent tank. The volume of the white oil or water is set as 5 μL, which is put on each plate, and then a camera record the profile of liquid drop.

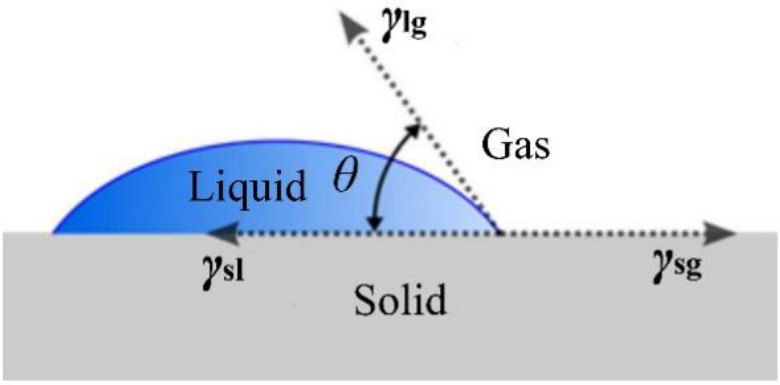


Figure 1. Schematic of the contact angle of a liquid drop.

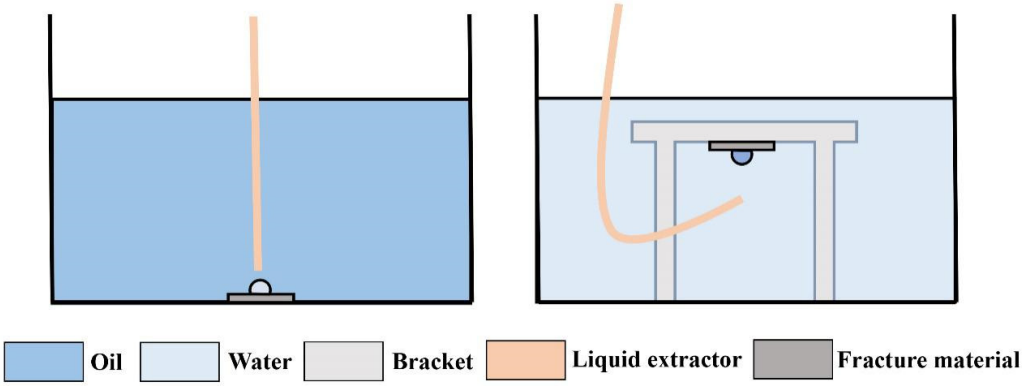


Figure 2. Schematic drawing for fluid 2–fluid 1–solid contact angle measurement.

In the experiment, water (ρ_w = 1000 kg/m^3, μ_w = 0.000987 Pa·s) and white oil (ρ_o = 810 kg/m^3, μ_o = 0.0098 Pa·s, μ_o/μ_w = 9.9) are working fluids at 23 °C and 0.101 MPa. The interfacial tension between oil and water measured by surface tension meter is 0.03 N/m. In the experiment, a fracture is initially saturated with water is called a water-saturated fracture, and a fracture is initially saturated with white oil is called an oil-saturated fracture. $\theta_{\text{fluid–solid–gas}}$ and $\theta_{\text{fluid 2–fluid 1–solid}}$ are contact angles for capillary fractures, as shown in Figure 3. $\theta_{\text{oil-gas–PMMA}}$, $\theta_{\text{water–gas–PMMA}}$ are 30.2° and 81.9°, respectively. $\theta_{\text{oil-gas–PTFE}}$, $\theta_{\text{water–gas–PTFE}}$ are 53.5°and 110.8°, respectively. These two materials are lipophilic and have different hydrophobic properties. $\theta_{\text{oil–water–PMMA}}$, $\theta_{\text{oil–water–PTFE}}$ are 77.2°and 82.1°, respectively. $\theta_{\text{water–oil–PMMA}}$, $\theta_{\text{water–oil–PTFE}}$ are 96.3°and 126.3°, respectively. It can be seen that $\theta_{\text{fluid 2–fluid 1–solid}}$ is greater than $\theta_{\text{fluid–solid–gas}}$. This is because that the surface of an oil-saturated or water-saturated solid is covered by liquid film which prevents

other liquid from contacting the surface of solid under the action of ionosphere and changes the static friction of surface contact [38].

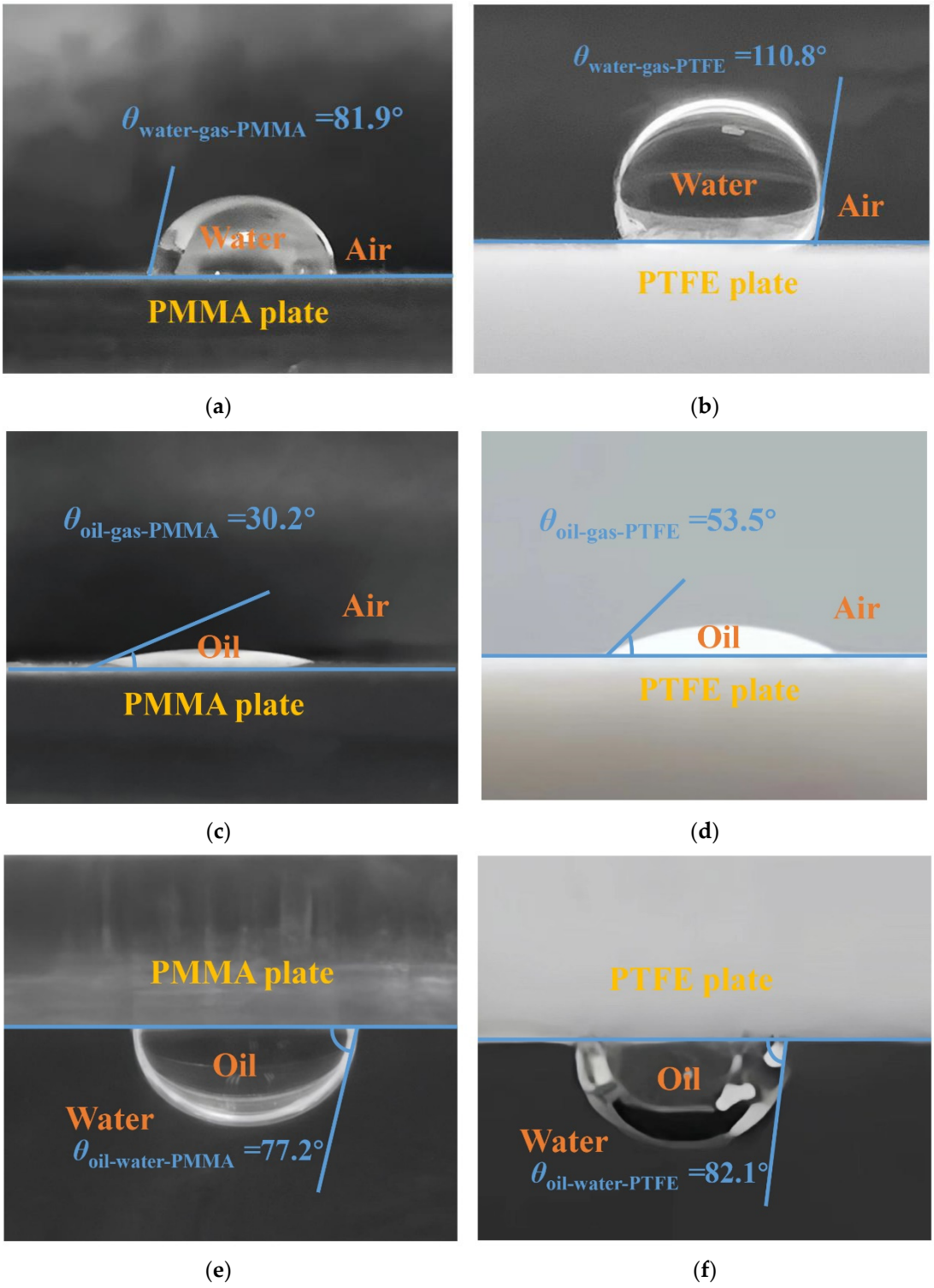
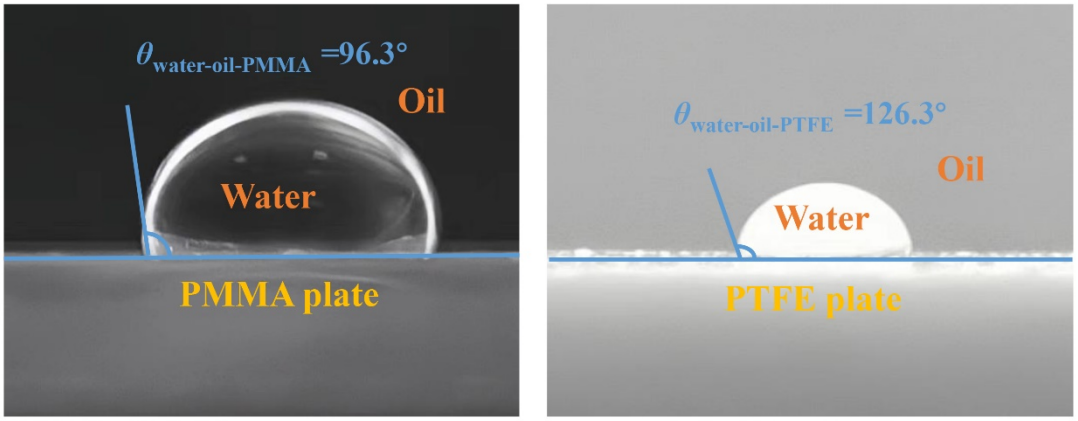


Figure 3. *Cont.*



(**g**) (**h**)

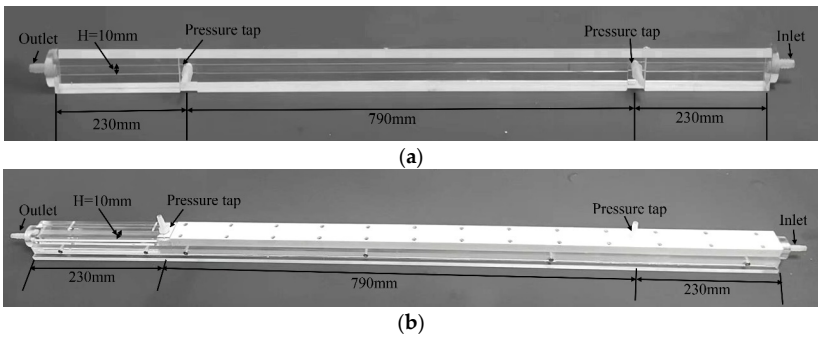
Figure 3. Contact angles of different materials. (**a**) $\theta_{water–gas–PMMA}$ = 81.9°. (**b**) $\theta_{water–gas–PTFE}$ = 110.8°. (**c**) $\theta_{oil–gas–PMMA}$ = 30.2°. (**d**) $\theta_{oil–gas–PTFE}$ = 53.5°. (**e**) $\theta_{oil–water–PMMA}$ = 77.2°. (**f**) $\theta_{oil–water–PTFE}$ = 82.1°. (**g**) $\theta_{water–oil–PMMA}$ = 96.3°. (**h**) $\theta_{water–oil–PTFE}$ = 126.3°.

3.2. Experimental Capillary Fractures

Two-phase flow in rectangular fractures is receiving increasing attention [39]. Experimental rectangular capillary fractures were fabricated in the polymethylmethacrylate (PMMA) plate and polytetrafluoroethylene (PTFE) plate by using micromachining technology. The total length of the rectangular capillary fracture is 1250 mm. Two pressure taps with a distance of 790 mm are machined on the rectangular capillary fracture, which are connected to pressure transmitters. The distance from the fracture inlet/outlet to the pressure tap is 230 mm. The heights *H* of the rectangular capillary fracture section are all 10 mm, and the widths *W* are 1.15 mm, 2.15 mm and 4 mm, respectively. The size of capillary fractures conforms to the scale characteristics of fractured reservoirs [40]. The detail dimensions of the rectangular capillary fractures are shown in Table 4. Due to the opacity of PTFE, there is a spliced PMMA fracture at the outlet of the experimental section of PTFE fracture, which is beneficial to observe water–oil flow regime in fractures. Experimental rectangular capillary fractures are shown in Figure 4.

Table 4. Dimensions of the rectangular capillary fractures.

Fracture	*W*/mm	*H*/mm	*H*/*W*	*A*/mm^2	*Po*	$k/\times 10^{-7}$ m^2	*B*/mm	d_h/mm
PTFE	1.15	10.0	8.7	11.5	83.28	1.02	22.3	2.06
PMMA	1.15	10.0	8.7	11.5	83.28	1.02	22.3	2.06
PMMA	2.15	10.0	4.7	21.5	75.23	3.33	24.3	3.54
PMMA	4	10.0	2.5	40	65.50	9.97	28	5.71



(**a**)

(**b**)

Figure 4. Experimental rectangular capillary fractures. (**a**) PMMA fracture. (**b**) PTFE fracture.

3.3. Experimental Setup

Figure 5 shows the experimental setup. Nitrogen cylinder serves as a power source to force water and white oil through horizontal capillary fractures. The total volume flowrate of oil and water flow was 10 L/h. In these rectangular capillary fractures, the water–oil flow was laminar and Reynolds numbers was between 2 and 1000. The oil flow rate and water flow rate were controlled by rotameters. All experimental parameters were recorded and measured under a new steady state. The experimental pressure drop range was 0.054 kPa–30 kPa, which was measured through a pressure transmitter. The uncertainties of flow rate, pressure drop, height and width were all 0.2%. The standard uncertainties of temperature was 0.1 °C. Absolute permeability k, the Poiseuille number Po and the hydraulic diameter of a fracture d_h, and the experimental relative permeabilities of water–oil flow (k_{rw} and k_{ro}) were calculated by Equations (1)–(5). From the uncertainty propagation law [41], in this experiment, the combined relative standard uncertainties of Po, k, k_{rw} and k_{ro} are 0.1%, 0.9%, 1.4% and 1.4%, respectively.

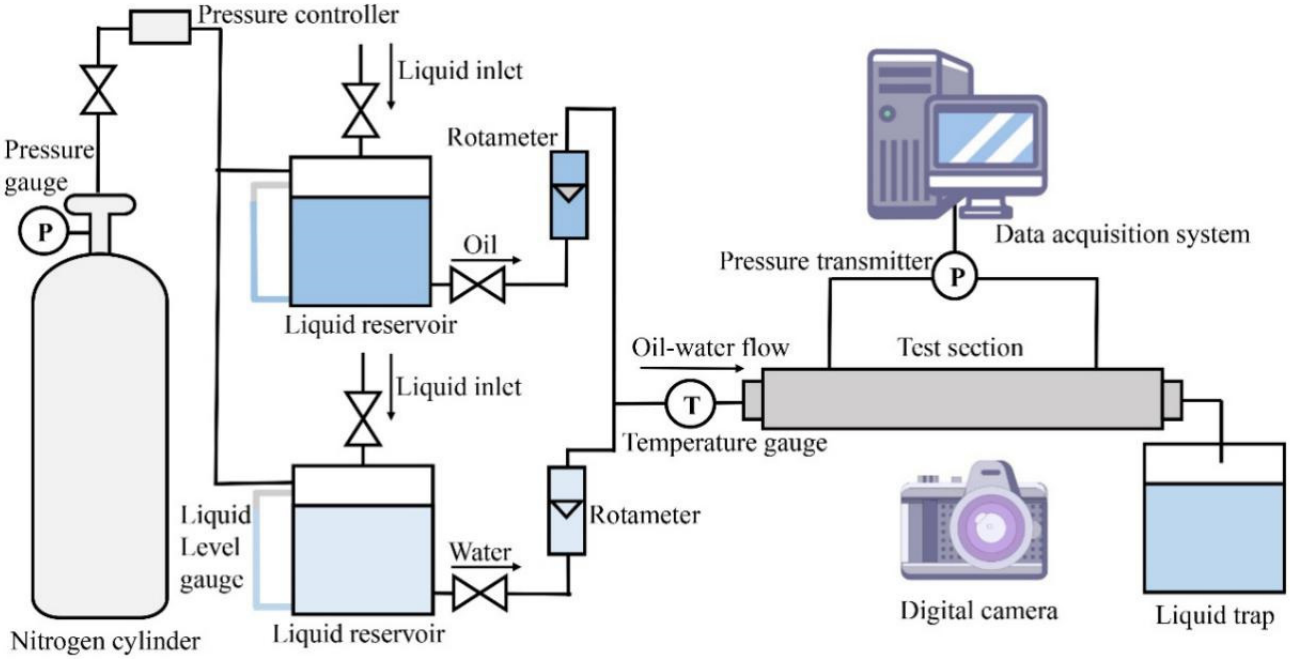
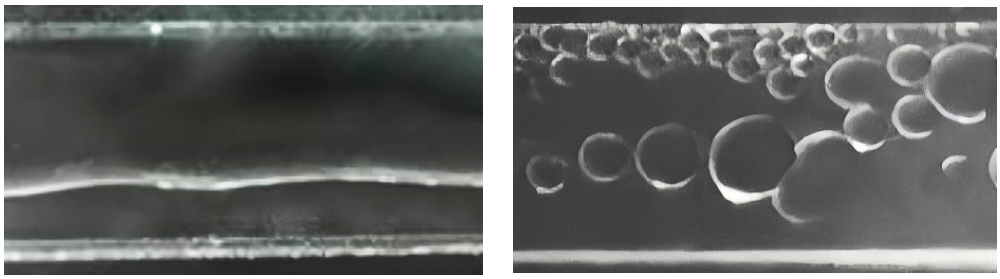


Figure 5. Experimental setup.

4. Results and Discussion

In this experiment, the water–oil flow was horizontal and laminar. Dispersed flow and stratified flow were observed in capillary fractures. These two flow regimes are shown in Figure 6. From Equations (4) and (5), the pressure drop of water–oil two-phase flow is crucial. The pressure drops of water–oil two-phase flow in water-saturated PMMA capillary fractures with hydraulic diameters of 2.06 mm, 3.54 mm and 5.71 mm are analyzed and verified firstly. The volumetric oil content of the transition from dispersed water–oil flow to stratified water–oil flow in capillary fractures with hydraulic diameters of 2.06 mm, 3.54 mm and 5.71 mm are 0.4, 0.5 and 0.53, respectively. The volumetric oil content of the transition from stratified water–oil flow to dispersed water–oil flow is 0.7.



(**a**) (**b**)

Figure 6. Flow regimes in capillary fractures. (**a**) Stratified flow. (**b**) Dispersed flow.

For stratified water–oil flow in a water-saturated PMMA capillary fracture, the oil phase is non-wetting fluid and water phase is wetting fluid. The comparison between the calculated pressure drops and the experimental ones for stratified water–oil flow in water-saturated PMMA capillary fractures is shown in Figure 7. The lines are the calculated results by Equations (6) and (7) without considering wettability while other marks are the experimental results. It shows that Equations (6) and (7) without considering wettability can well predict the pressure drop of stratified water–oil flow in water-saturated PMMA capillary fractures. That is to say, the relative permeabilities of stratified flow model without considering wettability can well predict the relative permeabilities of stratified water–oil flow in water-saturated PMMA capillary fractures.

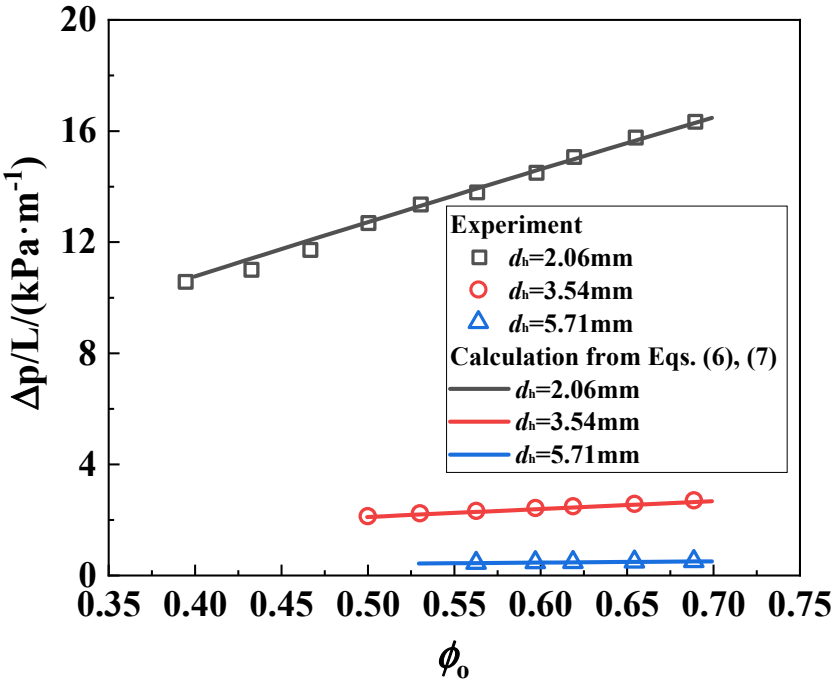


Figure 7. Comparison between the calculated pressure drops and the experimental ones for stratified water–oil flow in water-saturated PMMA capillary fractures ($\theta_{\text{oil–water–PMMA}} = 77.2^{\circ}$).

For dispersed water–oil flow, the experimental viscosity in a water-saturated PMMA capillary fracture with a hydraulic diameter of 2.06 mm is compared with the empirical viscosity models [42–44] in Figure 8a. The experimental values of viscosity are between the viscosity values calculated by these three empirical models. A new viscosity Equation (33) is proposed based on experimental viscosity and Brinkman model as below

$$\mu_{\text{r}} = (1-\phi_{\text{d}})^{-2.5}\left(0.001\frac{L}{d_{\text{h}}} + 2.865\phi_{\text{d}}\right) \tag{33}$$

where μ_r is the ratio of dynamic viscosity for dispersed flow to the dynamic viscosity of continuous phase; ϕ_d is the ratio of volumetric contents for the dispersed phase.

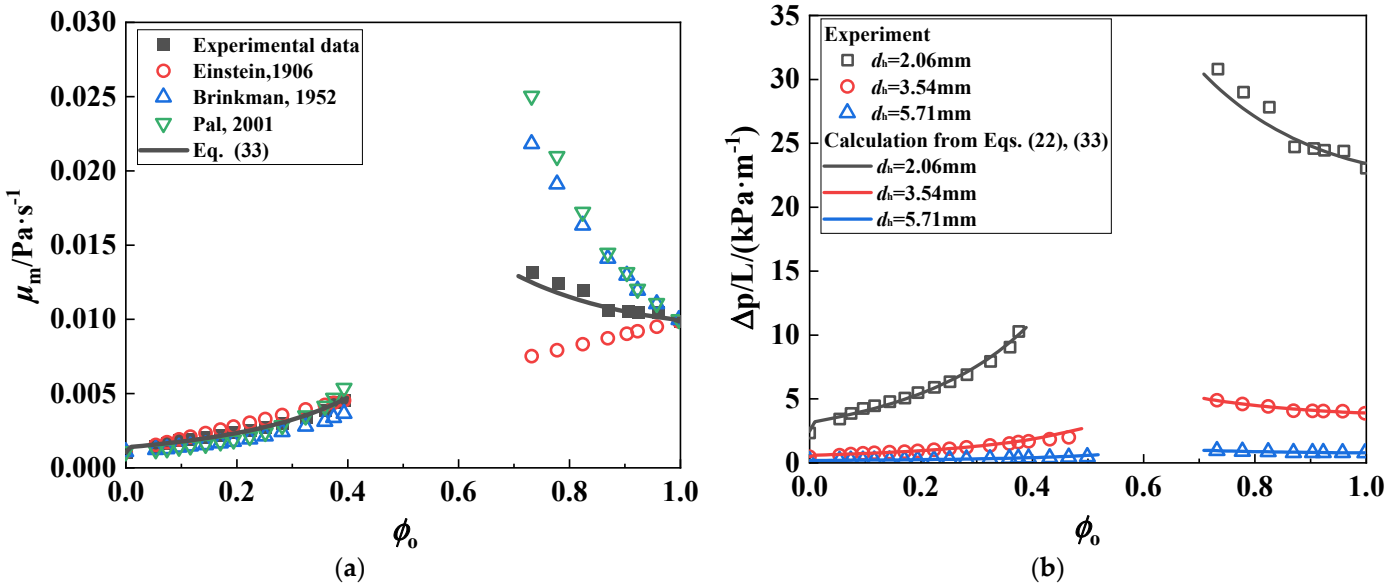


Figure 8. Comparison between the calculated data and the experimental ones for dispersed flow in water-saturated PMMA capillary fractures. (**a**) Viscosity in a water-saturated PMMA capillary fracture (d_h = 2.06 mm, $\theta_{oil-water-PMMA}$ = 77.2°) [42–44]. (**b**) Pressure drop in water-saturated PMMA capillary fractures with different hydraulic diameters ($\theta_{oil-water-PMMA}$ = 77.2°).

In Figure 8a, the new viscosity Equation (33) can well predict the viscosity for dispersed water–oil flow in a water-saturated PMMA capillary fracture. In Figure 8b, the lines are the calculated results by Equations (22) and (33) without considering wettability while other marks are the experimental results. It shows that the calculated pressure drops in water-saturated PMMA capillary fractures with different hydraulic diameters are consistent with the experimental pressure drops. So the relative permeabilities of dispersed flow model without considering wettability can well predict the relative permeabilities of dispersed flow in water-saturated PMMA capillary fractures.

Numerous experimental and simulation studies have shown that the state of wettability of tubes have an impact on water–oil two-phase flow There are few reports on the combination of theory and experiment to analyze the wettability effect on the relative permeabilities of water–oil flow. Therefore, based on the theoretical models of relative permeability developed in this paper, the relative permeabilities of water–oil two-phase flow have been investigated for different wettability situations such as water-saturated capillary fractures and oil-saturated capillary fractures made of different materials.

4.1. Relative Permeabilities in Saturated Capillary Fractures of Different Diameters

First, the relative permeabilities of water–oil two-phase flow in saturated PMMA capillary fractures with hydraulic diameters of 2.06 mm, 3.54 mm and 5.71 mm are analyzed. The results are illustrated in Figure 9.

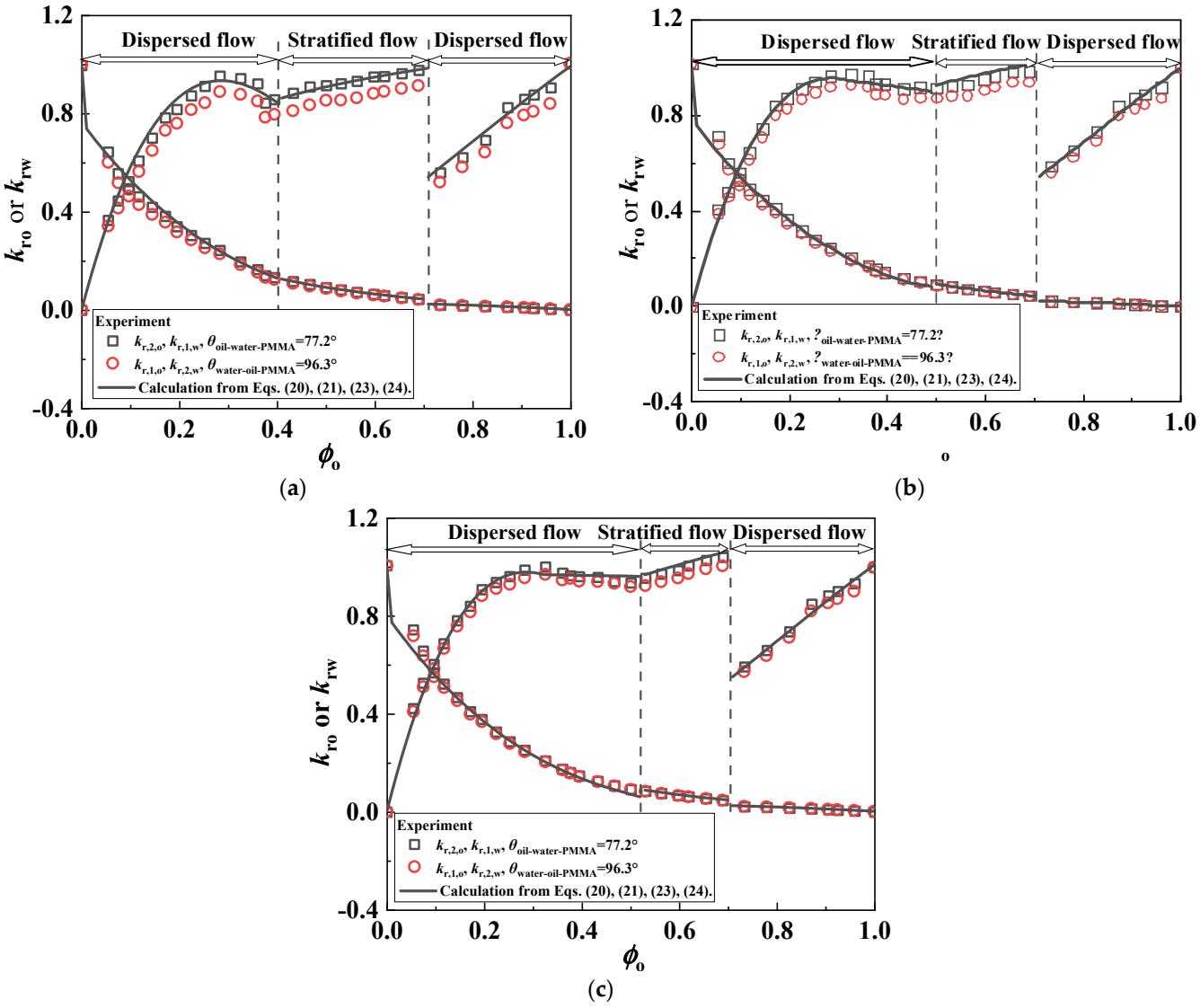


Figure 9. Relative permeabilities of water–oil two-phase flow in saturated PMMA capillary fractures with different hydraulic diameters: (**a**) d_h = 2.06 mm, (**b**) d_h = 3.54 mm, and (**c**) d_h = 5.71 mm.

As shown in Figure 9, the lines represent the calculated results of relative permeability models without considering wettability while other marks represent the experimental results. The relative permeability models without considering wettability can well predict the relative permeabilities of water–oil flow in water-saturated PMMA capillary fractures. The relative permeabilities of water–oil two-phase flow in a water-saturated PMMA capillary fracture are greater than those in an oil-saturated PMMA capillary fracture. As seen in Figure 3, $\theta_{\text{oil-gas–PMMA}}$, $\theta_{\text{water–gas–PMMA}}$ are 30.2° and 81.9°, respectively. PMMA is lipophilic and hydrophilic. The adsorption of oil makes the space for fluid to flow in the oil-saturated PMMA fracture smaller. Water film on a fracture is beneficial for fluid flow [15]. As also seen in Figure 3, $\theta_{\text{oil–water–PMMA}}$, $\theta_{\text{water–oil–PMMA}}$ are 77.2°and 96.3°, respectively. $\theta_{\text{oil–water–PMMA}} - \theta_{\text{oil-gas–PMMA}} > \theta_{\text{water–oil–PMMA}} - \theta_{\text{water–gas–PMMA}}$, water-saturated capillary fractures are advantageous to the flow of water–oil two-phase flow. In addition, the wettability effect on the relative permeabilities of water–oil two-phase flow increases as the hydraulic diameters of capillary fractures decrease. This can be explained that two fluids flow in a fracture with significantly interfering with each other and fracture surface when the fracture diameter is small, which is same as the conclusions of Yi [5].

Analysis of variance is used to study the relative permeabilities of water–oil two-phase flow in rectangular capillary fractures with different wettabilities [45]. The volumetric oil content and wettability situation are two factors that affect the relative permeabilities of water–oil two-phase flow. The degrees of freedom for volumetric oil content and wettability situation are 29 and 1, respectively. *F* critical values of for volumetric oil content and wettability situations at a significance level of 0.05 are 1.86 and 4.18, respectively. Table 5 shows that *F* values for the relative permeabilities of water–oil two-phase flow in saturated capillary fractures with hydraulic diameters of 2.06 mm, 3.54 mm and 5.71 mm are greater than F critical values, so the wettability of saturated fracture has an effect on the relative permeabilities of water–oil two-phase flow.

Table 5. F values for the relative permeabilities of water–oil two-phase flow in saturated PMMA capillary fractures with different hydraulic diameters.

Factors	*F* Values for Relative Permeabilities in Saturated PMMA Capillary Fractures						*F* Critical Values
	d_h = 2.06 mm		d_h = 3.54 mm		d_h = 5.71 mm		
	k_{ro}	k_{rw}	k_{ro}	k_{rw}	k_{ro}	k_{rw}	
Volumetric oil content	630.25	800.86	1648.28	1704.72	1950.27	3892.66	1.86
wettability situation	594.23	30.79	805.45	28.69	343.87	26.24	4.18

4.2. Relative Permeabilities in Saturated Capillary Fractures of Different Materials

Next, the relative permeabilities of water–oil flow in capillary fractures of different materials with the same hydraulic diameter of 2.06 mm are analyzed. Material types of fracture are selected: PTFE and PMMA. The results are illustrated in Figure 10.

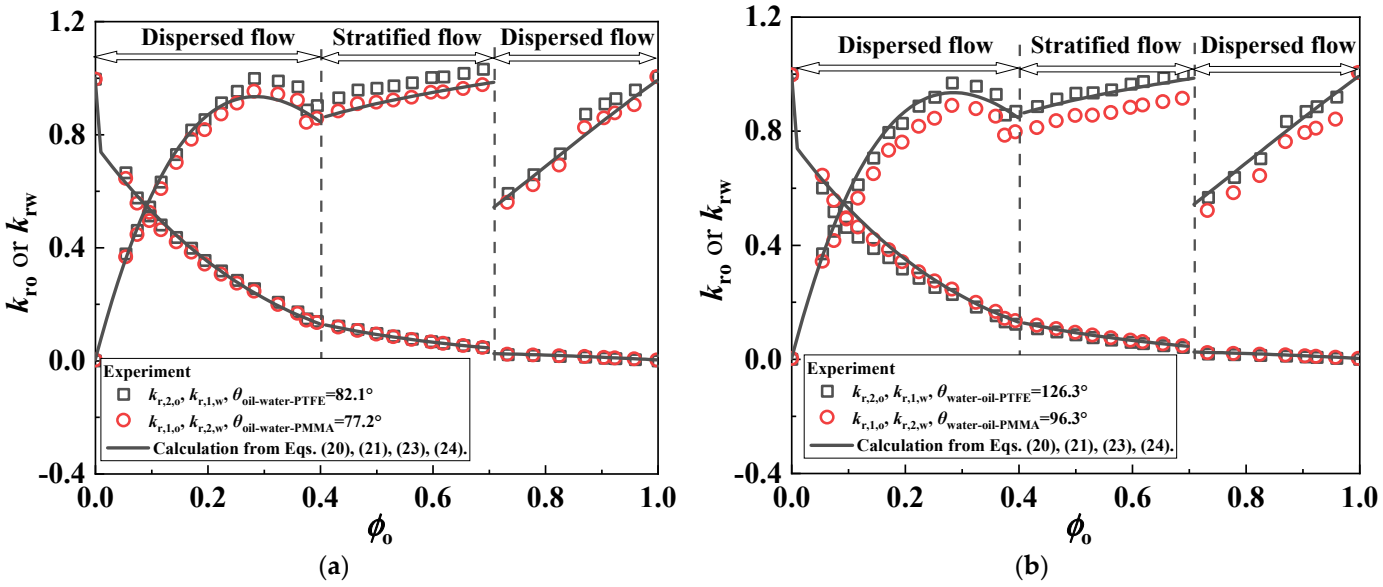


Figure 10. Relative permeabilities of water–oil two-phase flow in a saturated PTFE capillary fracture and a saturated PMMA capillary fracture with a hydraulic diameter of 2.06 mm. (**a**) Relative permeabilities in water-saturated capillary fractures of different materials; (**b**) Relative permeabilities in oil-saturated capillary fractures of different materials.

As shown in Figure 10, the relative permeability models without considering wettability can well predict the relative permeabilities of water–oil flow in a water-saturated PMMA capillary fracture and an oil-saturated PTFE fracture. The relative permeabilities of water–oil flow in a PFTE capillary fracture are larger than those in a PMMA capillary fracture. The wettability effect on the relative permeabilities of water–oil two-phase flow in an oil-saturated fracture is greater than that on the relative permeabilities of water–oil two-phase flow in a water-saturated fracture. As shown in Figure 3, $\theta_{oil\text{-}gas\text{–}PMMA}$, $\theta_{water\text{–}gas\text{–}PMMA}$ are 30.2° and

81.9°, respectively. $\theta_{\text{oil-gas–PTFE}}$, $\theta_{\text{water–gas–PTFE}}$ are 53.5°and 110.8°, respectively. PMMA is hydrophilic and PTFE is hydrophobic. PMMA is more lipophilic than PTFE. Hydrophobic capillary fractures are beneficial for fluid flow [46]. Therefore, water–oil two-phase flow can flow better in a PTFE capillary fracture. As also shown in Figure 3, $\theta_{\text{oil–water–PMMA}}$, $\theta_{\text{oil–water–PTFE}}$ are 77.2°and 82.1°, respectively. $\theta_{\text{water–oil–PMMA}}$, $\theta_{\text{water–oil–PTFE}}$ are 96.3°and 126.3°, respectively. $\theta_{\text{oil–water–PTFE}} - \theta_{\text{oil–water–PMMA}} < \theta_{\text{water–oil–PTFE}} - \theta_{\text{water–oil–PMMA}}$. As a result, the wettability has a significant impact on the relative permeability of water–oil two-phase flow in an oil-saturated capillary fracture. Table 6 also shows that F values for the relative permeabilities of water–oil two-phase flow in capillary fractures of different materials with a hydraulic diameter of 2.06 mm are greater than *F* critical values. That is to say, the wettability of fracture material has influence on the relative permeabilities of water–oil two-phase flow.

Table 6. F values for the relative permeabilities of water–oil two-phase flow in saturated capillary fractures of different materials with a hydraulic diameter of 2.06 mm.

Factors	*F* Values for Relative Permeabilities in Saturated Capillary Fractures of Different Materials				*F* Critical Values
	Water Saturated		Oil Saturated		
	k_{ro}	k_{rw}	k_{ro}	k_{rw}	
Volumetric oil content	860.20	3020.35	451.85	800.86	1.86
Wettability situation	384.41	41.52	603.99	30.79	4.18

4.3. Effect of Wettability on Relative Permeabilities

For the same flow regime, considering wettability or not will result in different relative permeability models. According to the relative permeability models considering wettability (Equations (14), (15), (26), and (27)), in the case $\frac{dp_c}{dx} = 0$ and $\frac{dS_2}{dx} = 0$, both c_1 and c_2 become 0. In the case $\frac{dp_c}{dx} \neq 0$ and $\frac{dS_2}{dx} \neq 0$, c_1 for stratified flow is associated with pressure drop per unit length, saturation of wetting fluid 1, $\frac{dp_c}{dx}$ and $\frac{dS_2}{dx}$. c_2 for stratified flow is related to pressure drop per unit length, capillary pressure, saturation of non-wetting fluid 2, $\frac{dp_c}{dx}$ and $\frac{dS_2}{dx}$. c_1 and c_2 for dispersed flow are both associated with saturation of wetting fluid 1, absolute permeability, average velocity for dispersed flow, dynamic viscosity for dispersed flow, $\frac{dp_c}{dx}$ and $\frac{dS_2}{dx}$. Figure 11 shows the effect of wettability on relative permeabilities.

Based on experimental relative permeabilities, Figure 11a, Equations (14), (15), (26) and (27), c_1 and c_2 are obtained, as shown in Figure 11b,c. It can be seen from Figure 11b,c, for water–oil flow in oil-saturated capillary fractures, c_{1o} ranges from −0.10 to 0.02 and c_{2w} ranges from −0.30 to 0.02. For water–oil flow in water-saturated capillary fractures, c_{2o} ranges from −0.01 to 0.05 and c_{1w} ranges from −0.01 to 0.05. Wettability can reduce the relative permeability of oil by a maximum of 10%, increase the relative permeability of oil by a maximum of 5%, reduce the relative permeability of water by a maximum of 30% and increase the relative permeability of water by a maximum of 5%. It also indicates that wettability has little effect on the permeability performances of water–oil two-phase flow in water-saturated capillary fractures, but is significant for those in oil-saturated capillary fractures. $\frac{dp_c}{dx}$ and $\frac{dS_2}{dx}$ are different in capillary fractures of different wettabilities. As also shown in Figure 3, PTFE and PMMA are oleophilic materials. Oil droplets are more easily sticky on the surfaces of capillary fractures than water droplets, resulting in the different effects of wettability on the permeability performance of water–oil two-phase flow in water-saturated capillary fractures and oil-saturated capillary fractures.

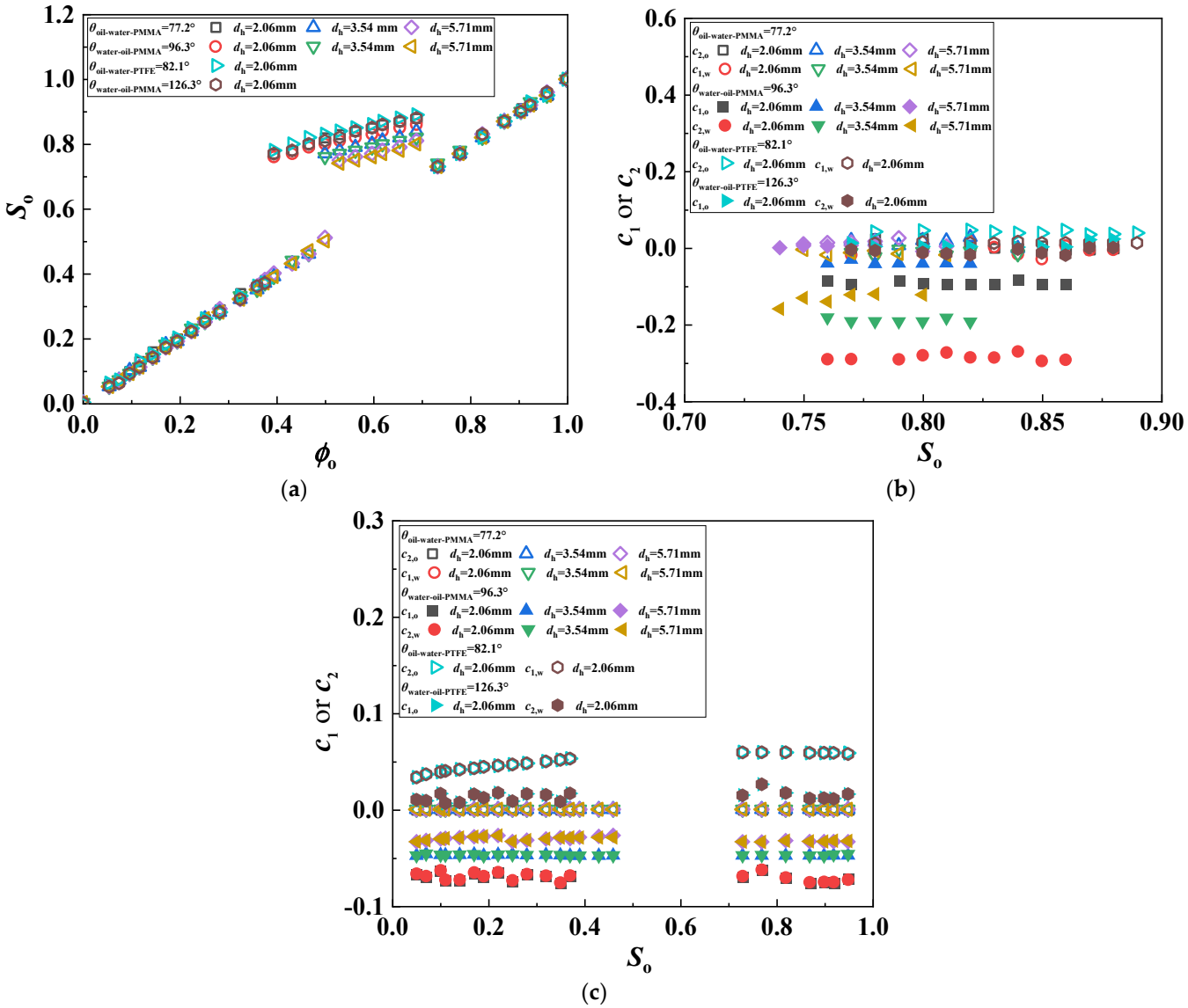


Figure 11. Effect of wettability on the relative permeabilities of water–oil two-phase flow in capillary fractures with different wettabilities. (**a**) Relationship between oil saturation and oil volumetric content. (**b**) c_1 and c_2 for stratified flow. (**c**) c_1 and c_2 for dispersed flow.

5. Conclusions

Based on the momentum equations of the two-fluid model with considering wall shear stresses, interfacial shear stress and capillary force, the relative permeability models with considering wettability were developed for dispersed flow and stratified flow. Experiments were conducted to study the relative permeabilities of laminar water–oil two-phase flow in water-saturated and oil-saturated horizontal capillary fractures with different hydraulic diameters. The main conclusions are as below:

(1) The relative permeabilities of stratified water–oil flow are relevant to wetted perimeter, saturation, interfacial slip coefficient and wettability coefficient. The relative permeabilities of dispersed water–oil flow hinge on saturation, viscosity and wettability coefficient.

(2) Wettability coefficients are proposed to study the wettability effect on the relative permeabilities of water–oil flow. Wettability has little effect on the permeability performances of water–oil two-phase flow in water-saturated capillary fractures, but is significant for those in the oil-saturated capillary fractures.

(3) The relative permeabilities of water–oil two-phase flow in a water-saturated capillary fracture are higher than those in an oil-saturated capillary fracture of the same material. As the hydraulic diameter of capillary fractures decreases, the influence of wettability on the relative permeabilities of water–oil two-phase flow increases. The relative permeabilities of water–oil two-phase flow in a PTFE capillary fracture are larger than those in a PMMA capillary fracture for the same saturated condition.
(4) Both theoretical models and analysis of variance on experimental data show that wettability has an influence on the relative permeabilities.

Author Contributions: Validation, N.H., H.C. and Y.H.; Formal analysis, N.H.; Investigation, H.C. and Y.H.; Resources, L.L.; Writing—original draft, N.H.; Writing—review & editing, N.H. and L.L.; Project administration, L.L.; Funding acquisition, L.L. All authors have read and agreed to the published version of the manuscript.

Funding: This research was funded by the National Natural Science Foundation of China: 11572241.

Data Availability Statement: The original contributions presented in the study are included in the article, further inquiries can be directed to the corresponding authors.

Conflicts of Interest: The authors declare that they have no known competing financial interests or personal relationships that could have appeared to influence the work reported in this paper.

References

1. Dragila, M.I.; Weisbrod, N. Fluid motion through an unsaturated fracture junction. *Water Resour. Res.* **2004**, *40*, 2403. [CrossRef]
2. Moodie, N.; Ampomah, W.; Jia, W.; McPherson, B. Relative permeability: A critical parameter in numerical simulations of multiphase flow in porous media. *Energies* **2021**, *14*, 2370. [CrossRef]
3. Su, Y.L.; Xu, J.L.; Wang, W.D.; Wang, H.; Zhan, S.Y. Relative permeability estimation of oil−water two-phase flow in shale reservoir. *Petrol. Sci.* **2022**, *19*, 1153–1164. [CrossRef]
4. Wu, K.; Chen, Z.; Li, J.; Li, X.; Xu, J.; Dong, X. Wettability effect on nanoconfined water flow. *Proc. Natl. Acad. Sci. USA* **2017**, *114*, 3358–3363. [CrossRef] [PubMed]
5. Yi, J.; Liu, L.; Xia, Z.; Wang, J.; Jing, Y.; Duan, L. Effects of wettability on relative permeability of rough-walled fracture at pore-scale: A lattice boltzmann analysis. *Appl. Therm. Eng.* **2021**, *194*, 117100. [CrossRef]
6. Zhang, Y.; Zeng, J.; Qiao, J.; Feng, X.; Dong, Y. Investigating the effect of the temperature and pressure on wettability in crude oil–brine–rock systems. *Energy Fuels* **2018**, *32*, 9010–9019. [CrossRef]
7. Mirzaei-Paiaman, A.; Faramarzi-Palangar, M.; Djezzar, S.; Kord, S. A new approach to measure wettability by relative permeability measurements. *J. Petrol. Sci. Eng.* **2022**, *208*, 109191. [CrossRef]
8. Ghedan, S.G.; Canbaz, C.H.; Boyd, D.A.; Mani, G.M.; Haggag, M.K. Wettability profile of a thick carbonate reservoir by the new rise in core wettability characterization method. In Proceedings of the Abu Dhabi International Petroleum Exhibition and Conference, Abu Dhabi, United Arab Emirates, 1–4 November 2010; pp. 1–4. [CrossRef]
9. Liu, Y.; Upchurch, E.R.; Ozbayoglu, E.M. Experimental and theoretical studies on taylor bubbles rising in stagnant non-newtonian fluids in inclined non-concentric annuli. *Int. J. Multiph. Flow* **2022**, *147*, 103912. [CrossRef]
10. Liu, Y.; Upchurch, E.R.; Ozbayoglu, E.M. Experimental study of single taylor bubble rising in stagnant and downward flowing non-newtonian fluids in inclined pipes. *Energies* **2021**, *14*, 578. [CrossRef]
11. Kumar, A.; Mandal, A. Critical investigation of zwitterionic surfactant for enhanced oil recovery from both sandstone and carbonate reservoirs: Adsorption, wettability alteration and imbibition studies. *Chem. Eng. Sci.* **2019**, *209*, 115222. [CrossRef]
12. Zhao, B.; MacMinn, C.W.; Juanes, R. Wettability control on multiphase flow in patterned microfluidics. *Proc. Natl. Acad. Sci. USA* **2016**, *113*, 10251–10256. [CrossRef]
13. Paolinelli, L.D.; Rashedi, A.; Yao, J.; Singer, M. Study of water wetting and water layer thickness in oil-water flow in horizontal pipes with different wettability. *Chem. Eng. Sci.* **2018**, *183*, 200–214. [CrossRef]
14. Riley, G.A.; Bultongez, K.K.; Derby, M.M. Oil-water flow regimes in 4-mm borosilicate glass and fluorinated ethylene propylene channels: Effects of wall wettability. *J. Petrol. Sci. Eng.* **2019**, *173*, 469–477. [CrossRef]
15. Prakash, R.; Ghosh, S. Effect of jump in wettability on the hydrodynamics of liquid–liquid two-phase flow in a straight mini capillary tube. *Chem. Eng. J.* **2022**, *435*, 135194. [CrossRef]
16. Oyenowo, O.P.; Wang, H.; Mirzaei-Paiaman, A.; Carrasco-Jaim, O.A.; Sheng, K.; Okuno, R. Geochemical impact of high-concentration formate solution injection on rock wettability for enhanced oil recovery and geologic carbon storage. *Energy Fuels* **2024**, *38*, 6138–6155. [CrossRef]
17. Al-Futaisi, A.; Patzek, T.W. Impact of wettability alteration on two-phase flow characteristics of sandstones: A quasi-static description. *Water Resour. Res.* **2003**, *39*, 1042. [CrossRef]

18. Zhao, X.; Blunt, M.J.; Yao, J. Pore-scale modeling: Effects of wettability on waterflood oil recovery. *J. Petrol. Sci. Eng.* **2010**, *71*, 169–178. [CrossRef]
19. Ryazanov, A.V.; Sorbie, K.S.; van Dijke, M.I.J. Structure of residual oil as a function of wettability using pore-network modelling. *Adv. Water Resour.* **2014**, *63*, 11–21. [CrossRef]
20. Zhao, J.; Kang, Q.; Yao, J.; Viswanathan, H.; Pawar, R.; Zhang, L.; Sun, H. The effect of wettability heterogeneity on relative permeability of two-phase flow in porous media: A lattice boltzmann study. *Water Resour. Res.* **2018**, *54*, 1295–1311. [CrossRef]
21. Cheng, L.; Li, X.; Rong, G.; Zhou, C. The effect of surface wettability and wall roughness on the residual saturation for the drainage process in sinusoidal channels. *Transp. Porous Media* **2019**, *129*, 203–229. [CrossRef]
22. Lee, C.Y.; Lee, S.Y. Influence of surface wettability on transition of two-phase flow pattern in round mini-channels. *Int. J. Multiphas Flow* **2008**, *34*, 706–711. [CrossRef]
23. Flipo, G.; Josset, C.; Bellettre, J.; Auvity, B. Clarification of the surface wettability effects on two-phase flow patterns in pemfc gas channels. *Int. J. Hydrogen Energy* **2016**, *41*, 15518–15527. [CrossRef]
24. Yagodnitsyna, A.A.; Kovalev, A.V.; Bilsky, A.V. Flow patterns of immiscible liquid-liquid flow in a rectangular microchannel with t-junction. *Chem. Eng. J.* **2016**, *303*, 547–554. [CrossRef]
25. Chinnov, E.; Ron'Shin, F.; Kabov, O.A. Two-phase flow patterns in short horizontal rectangular microchannels. *Int. J. Multiph. Flow* **2016**, *80*, 57–68. [CrossRef]
26. Ganguli, A.A.; Pandit, A.B. Hydrodynamics of liquid-liquid flows in micro channels and its influence on transport properties: A review. *Energies* **2021**, *14*, 6066. [CrossRef]
27. Moezzi, M.; Hannani, S.K.; Farhanieh, B. Hysteretic heat transfer study of liquid–liquid two-phase flow in a t-junction microchannel. *Int. J. Heat Fluid Flow* **2019**, *77*, 366–376. [CrossRef]
28. Al-Azzawi, M.; Mjalli, F.S.; Husain, A.; Al-Dahhan, M. A review on the hydrodynamics of the liquid-liquid two-phase flow in the microchannels. *Ind. Eng. Chem. Res.* **2021**, *60*, 5049–5075. [CrossRef]
29. Zhao, Y.C.; Chen, G.W.; Yuan, Q. Liquid-liquid two-phase flow patterns in a rectangular microchannel. *AIChE J.* **2006**, *52*, 4052–4060. [CrossRef]
30. Huang, N.; Liu, L.; Zhang, X.; Ma, K.; Zhou, M.W. Analytical models and experimental verifications for relative permeabilities of oil-water two-phase flow in fractures. *Petrol. Sci. Technol.* **2023**, 1–25. [CrossRef]
31. Shah, R.K.; London, A.L.; White, F.M. Laminar flow forced convection in ducts. *J. Fluid Eng.* **1980**, *102*, 431–455. [CrossRef]
32. Higdon, J.J.L. Multiphase flow in porous media. *J. Fluid Mech.* **2013**, *730*, 1–4. [CrossRef]
33. Jia, K.; Zeng, J.; Wang, X.; Li, B.; Gao, X.; Wang, K. Wettability of tight sandstone reservoir and its impacts on the oil migration and accumulation: A case study of shahejie formation in dongying depression, bohai bay basin. *Energies* **2022**, *15*, 4267. [CrossRef]
34. Lahey, R.T. Wave propagation phenomena in two-phase flow. In *Boiling Heat Transfer*; Elsevier: Amsterdam, The Netherlands, 1992; pp. 123–173. [CrossRef]
35. Brauner, N.; Maron, D.M.; Rovinsky, J. A two-fluid model for stratified flows with curved interfaces. *Int. J. Multiph. Flow* **1998**, *24*, 975–1004. [CrossRef]
36. Santos, D.S.; Faia, P.M.; Garcia, F.A.P.; Rasteiro, M.G. Experimental and simulated studies of oil/water fully dispersed flow in a horizontal pipe. *J. Fluid Eng.* **2019**, *141*, 111301. [CrossRef]
37. Young, T. An essay on the cohesion of fluids. *Philos. Trans. R. Soc. Lond.* **1805**, *95*, 65–87. [CrossRef]
38. Tian, X.; Bhushan, B. The micro-meniscus effect of a thin liquid film on the static friction of rough surface contact. *J. Phys. D Appl. Phys.* **1996**, *29*, 163. [CrossRef]
39. Bertels, S.P.; Dicarlo, D.A.; Blunt, M.J. Measurement of aperture distribution, capillary pressure, relative permeability, and in situ saturation in a rock fracture using computed tomography scanning. *Water Resour. Res.* **2001**, *37*, 649–662. [CrossRef]
40. Hashimoto, M.; Garstecki, P.; Stone, H.A.; Whitesides, G.M.J.S.M. Interfacial instabilities in a microfluidic hele-shaw cell. *Soft Matter* **2008**, *4*, 1403–1413. [CrossRef]
41. Iso, E. Guide to the expression of uncertainty in measurement. *Meas. Uncertain.* **2008**, *30*, 105–107. [CrossRef]
42. Brinkmann, H.C. The viscosity of concentraed suspensions and solutions. *J. Chem. Phys.* **1952**, *20*, 571. [CrossRef]
43. Pal, R. Viscosity–concentration equation for emulsions of nearly spherical droplets. *J. Colloid Interface Sci.* **2001**, *231*, 168–175. [CrossRef] [PubMed]
44. Einstein, A. Eine neue bestimmung der moleküldimensionen. *Ann. Phys.* **1905**, *19*, 289–306. [CrossRef]
45. Srivastava, M. Analysis of variance and covariance. *J. Appl. Stat.* **2010**, *37*, 1781–1782. [CrossRef]
46. Ou, J.; Perot, B.; Rothstein, J.P. Laminar drag reduction in microchannels using ultrahydrophobic surfaces. *Phys. Fluid* **2004**, *16*, 4635–4643. [CrossRef]

Disclaimer/Publisher's Note: The statements, opinions and data contained in all publications are solely those of the individual author(s) and contributor(s) and not of MDPI and/or the editor(s). MDPI and/or the editor(s) disclaim responsibility for any injury to people or property resulting from any ideas, methods, instructions or products referred to in the content.